ARMY RESEARCH LABORATORY

Linear Theory of a Dual-Spin Projectile in Atmospheric Flight

by Mark F. Costello
and Allen A. Peterson

ARL-CR-448 February 2000

The findings in this report are not to be construed as an official Department of the Army position unless so designated by other authorized documents.

Citation of manufacturer's or trade names does not constitute an official endorsement or approval of the use thereof.

Destroy this report when it is no longer needed. Do not return it to the originator.

ERRATA SHEET

re: ARL-CR-448, "Linear Theory of a Dual-Spin Projectile in Atmospheric Flight," by Mark F. Costello and Allen A. Peterson

Request the following pen-and-ink changes be made to page 47.

Block 4: Linear Theory of a Dual-Spin Projectile n Atmospheric Flight

Change to read: Linear Theory of a Dual-Spin Projectile in Atmospheric Flight

Block 14: Add the following subject terms:

flight dynamics, dual-spin, projectile

Army Research Laboratory
Aberdeen Proving Ground, MD 21005-5066

ARL-CR-448 **February 2000**

Linear Theory of a Dual-Spin Projectile in Atmospheric Flight

Mark F. Costello and Allen A. Peterson
Weapons and Materials Research Directorate, ARL

Abstract

The equations of motion for a dual-spin projectile in atmospheric flight are developed and subsequently utilized to solve for angle of attack and swerving dynamics. A combination hydrodynamic and roller bearing couples forward and aft body roll motions. Using a modified projectile linear theory developed for this configuration, it is shown that the dynamic stability factor, S_D, and the gyroscopic stability factor, S_G, are altered compared to a similar rigid projectile, due to new epicyclic fast and slow arm equations. Swerving dynamics including aerodynamic jump are studied using the linear theory.

Table of Contents

INTENTIONALLY LEFT BLANK.

List of Figures

INTENTIONALLY LEFT BLANK.

List of Symbols

x, y, z	Position vector components of the composite center of mass expressed in the inertial reference frame.
θ , ψ	Euler pitch, and yaw angles.
ϕ_F	Euler roll angle of the forward body.
ϕ_A	Euler roll angle of the aft body.
u, v, w	Translation velocity components of the composite center of mass resolved in the fixed plane reference frame.
p_F	Roll axis component of the angular velocity vector of the forward body expressed in the fixed plane reference frame.
p_A	Roll axis component of the angular velocity vector of the aft body expressed in the fixed plane reference frame.
q, r	Components of the angular velocity vector of both the forward and aft bodies expressed in the fixed plane reference frame.
X, Y, Z	Total external force components on the composite body expressed in the fixed plane reference frame.
L_F, M_F, N_F	External moment components on the forward body expressed in the fixed plane reference frame.
L_A, M_A, N_A	External moment components on the aft body expressed in the fixed plane reference frame.
m_F	Forward body mass.
m_A	Aft body mass.
m	Total projectile mass.
I_F	Mass moment of inertia matrix of the forward body with respect to the forward body reference frame.

I_A	Mass moment of inertia matrix of the aft body with respect to the aft body reference frame.
I	Effective inertia matrix.
D	Projectile characteristic length.
C_i	Various projectile aerodynamic coefficients.
q_a	Dynamic pressure at the projectile mass center.
α	Longitudinal aerodynamic angle of attack.
β	Lateral aerodynamic angle of attack.
V	Magnitude of mass center velocity.
T_F	Transformation matrix from the fixed plane reference frame to the forward body reference frame.
T_A	Transformation matrix from the fixed plane reference frame to the aft body reference frame.
$\vec{i}_n, \vec{j}_n, \vec{k}_n$	Fixed plane unit vectors.
c_V	Viscous damping coefficient for hydrodynamic bearing.
c_{RB}	Friction coefficient for roller bearing.
r_{fx}, r_{fy}, r_{fz}	Fixed plane components of vector from composite center of mass to forward body mass center.
r_{ax}, r_{ay}, r_{az}	Fixed plane components of vector from composite center of mass to aft body mass center.
$\bar{r}$	Vector from composite center of mass to central bearing.
R_{fx}, R_{fy}, R_{fz}	Fixed plane components of vector from forward body mass center to forward body center of pressure.

R_{ax}, R_{ay}, R_{az} Fixed plane components of vector from aft body mass center to aft body center of pressure.

$Rm_{fx}, Rm_{fy}, Rm_{fz}$ Fixed plane components of vector from forward body mass center to forward body Magnus center of pressure.

$Rm_{ax}, Rm_{ay}, Rm_{az}$ Fixed plane components of vector from aft body mass center to aft body Magnus center of pressure.

INTENTIONALLY LEFT BLANK.

1. Introduction

Compared to conventional munitions, the design of smart munitions involves more design requirements stemming from the addition of sensors and control mechanisms. The addition of these components must seek to minimize the weight and space impact on the overall projectile design so that desired target effects can still be achieved with the weapon. The inherent design conflict between standard projectile design considerations and new requirements imposed by sensors and control mechanisms has led designers to consider more complex geometric configurations. One such configuration is the dual-spin projectile. This projectile configuration is composed of forward and aft components. The forward and aft components are connected through a bearing, which allows the forward and aft portions of the projectile to spin at different rates. Figure 1 shows a schematic of this projectile configuration.

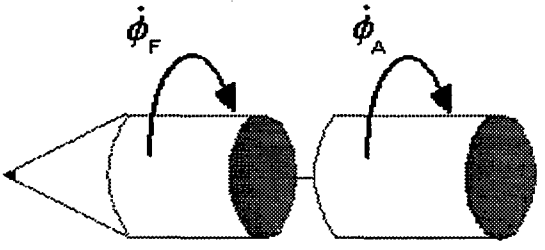

Figure 1. Dual-Spin Projectile Schematic.

Dual-spin spacecraft dynamics have been extensively studied in the literature. For example, Likins [1] studied the motion of a dual-spin spacecraft and conditions for stability were established. Later, Cloutier [2] obtained an analytical criterion for infinitesimal stability. Along these lines, Mingori [3] as well as Fang [4] considered energy dissipation. Hall and Rand [5] considered spinup dynamics, and resonances occurring during despin were studied by Or [6]. In the latter, the linear equations governing the resonance dynamics were found to depend on nondimensional parameters related to dynamic unbalance, asymmetry, and the time duration for resonance growth. Other work investigating asymmetric mass properties is due to Cochran, Shu, and Rew [7] as well as Tsuchiya [8] and Yang [9]. Viderman, Rimrott, and Cleghorn [10]

developed a dynamic model of a dual-spin spacecraft with a flexible platform. Stability was investigated using Floquet theory. Stabb and Schlack [11] investigated pointing accuracy of a dual-spin spacecraft using the Krylov-Bogoliubov-Mitropolsky perturbation method.

For projectile flight in the atmosphere, aerodynamic forces and moments play a dominant role in the dynamic characteristics. These effects have obviously not been considered in the dual-spin spacecraft efforts described previously. However, Smith, Smith, and Topliffe [12] considered the dynamics of a spin-stabilized artillery projectile modified to accommodate controllable canards mounted to the projectile by a bearing aligned with the spin axis. This work focused on the use of actively controlled canards to reduce miss distance. Both the forward and aft bodies were mass balanced and a hydrodynamic bearing coupled forward and aft body rolling motion.

The dual-spin projectile model developed here permits nonsymmetric forward and aft body components and allows a combination of hydrodynamic and roller bearing roll coupling between the forward and aft bodies. By applying the linear theory for a rigid projectile in atmospheric flight, a dual-spin projectile linear theory is developed. Expressions for the gyroscopic and dynamic stability factor are developed and compared to the rigid projectile case. The swerving motion of this configuration is also considered.

2. Dual-Spin Projectile Dynamic Model

The mathematical model describing the motion of the dual-spin projectile allows for three translation and four rotation rigid body degrees of freedom (DOF). The translation degrees of freedom are the three components of the mass center position vector. The rotation degrees of freedom are the Euler yaw and pitch angles as well as the forward body roll and aft body roll angles. The ground surface is used as an inertial reference frame [13].

Development of the kinematic and dynamic equations of motion is aided by the use of an intermediate reference frame. The sequence of rotations from the inertial frame to the forward and aft bodies consists of a set of body fixed rotations that are ordered: yaw, pitch, and

forward/aft body roll. The fixed plane reference frame is defined as the intermediate frame before roll rotation. The fixed plane frame is convenient because both the forward and aft bodies share this frame before roll rotation.

Equations 1–4 represent the translation and rotation kinematic and dynamic equations of motion for a dual-spin projectile. Both sets of dynamic equations are expressed in the fixed plane reference frame.

$$\begin{Bmatrix} \dot{x} \\ \dot{y} \\ \dot{z} \end{Bmatrix} = \begin{bmatrix} c_\theta c_\psi & -s_\psi & s_\theta c_\psi \\ c_\theta s_\psi & c_\psi & s_\theta s_\psi \\ -s_\theta & 0 & c_\theta \end{bmatrix} \begin{Bmatrix} u \\ v \\ w \end{Bmatrix} \tag{1}$$

$$\begin{Bmatrix} \dot{\phi}_F \\ \dot{\phi}_A \\ \dot{\theta} \\ \dot{\psi} \end{Bmatrix} = \begin{bmatrix} 1 & 0 & 0 & t_\theta \\ 0 & 1 & 0 & t_\theta \\ 0 & 0 & 1 & 0 \\ 0 & 0 & 0 & 1/c_\theta \end{bmatrix} \begin{Bmatrix} p_F \\ p_A \\ q \\ r \end{Bmatrix} \tag{2}$$

$$\begin{Bmatrix} \dot{u} \\ \dot{v} \\ \dot{w} \end{Bmatrix} = \begin{Bmatrix} \frac{X}{m} \\ \frac{Y}{m} \\ \frac{Z}{m} \end{Bmatrix} - \begin{bmatrix} 0 & -r & q \\ r & 0 & rt_\theta \\ -q & -rt_\theta & 0 \end{bmatrix} \begin{Bmatrix} u \\ v \\ w \end{Bmatrix} \tag{3}$$

$$\begin{Bmatrix} \dot{p}_F \\ \dot{p}_A \\ \dot{q} \\ \dot{r} \end{Bmatrix} = [I]^{-1} \begin{Bmatrix} g_{F1} - M_V \\ g_{A1} + M_V \\ M_2 - S_2^* \\ M_3 - S_3^* \end{Bmatrix} \tag{4}$$

A derivation of equation 4 is provided in the Appendix.

Loads on the composite projectile body are due to weight and aerodynamic forces acting on both the forward and aft bodies. Equations 5 and 6 provide expressions for the forward body weight and aerodynamic forces.

$$\begin{Bmatrix} X_W^F \\ Y_W^F \\ Z_W^F \end{Bmatrix} = m_F g \begin{Bmatrix} -s_\theta \\ 0 \\ c_\theta \end{Bmatrix} \tag{5}$$

$$\begin{Bmatrix} X_A^F \\ Y_A^F \\ Z_A^F \end{Bmatrix} = -\tilde{q}_a \begin{Bmatrix} C_{X0}^F + C_{XA2}^F \alpha^2 + C_{XB2}^F \beta^2 \\ C_{Y0}^F + C_{YB1}^F \beta \\ C_{Z0}^F + C_{ZA1}^F \alpha \end{Bmatrix} \tag{6}$$

Linear Magnus forces acting on the forward body are formulated separately in equation 7. These forces act at the Magnus force center of pressure, which is different from the center of pressure of the steady aerodynamic forces.

$$\begin{Bmatrix} X_M^F \\ Y_M^F \\ Z_M^F \end{Bmatrix} = \tilde{q}_a \begin{Bmatrix} 0 \\ \dfrac{p_F D C_{NPA}^F \alpha}{2V} \\ -\dfrac{p_F D C_{NPA}^F \beta}{2V} \end{Bmatrix} \tag{7}$$

The longitudinal and lateral aerodynamic angles of attack used in equations 6 and 7 are computed using equation 8.

$$\alpha = \tan^{-1}\left(\frac{w}{u}\right) \qquad \beta = tan^{-1}\left(\frac{v}{u}\right) \tag{8}$$

$$\tilde{q}_a = \frac{1}{8}\rho(u^2 + v^2 + w^2)\pi D^2 \tag{9}$$

Expressions for the aft body forces take on the same form. Aerodynamic coefficients in equations 6 and 7 depend on the local Mach number at the projectile mass center. They are computed using linear interpolation from a table of data.

The right-hand side of the rotation kinetic equations contains the externally applied moments on both the forward and aft bodies. These equations contain contributions from steady and unsteady aerodynamics. The steady aerodynamic moments are computed for each individual body with a cross product between the steady body aerodynamic force vector and the distance vector from the center of gravity to the center of pressure. Magnus moments on each body are computed in a similar way, with a cross product between the Magnus force vector and the distance vector from the center of gravity to the Magnus center of pressure. Figure 2 shows the relative locations of the forward, aft, and composite body centers of gravity and the forward and aft body centers of pressure. The unsteady body aerodynamic moments provide a damping source for projectile angular motion and are given for the forward body by equation 10.

$$\begin{Bmatrix} L_{UA}^{F} \\ M_{UA}^{F} \\ N_{UA}^{F} \end{Bmatrix} = \tilde{q}_a D \begin{Bmatrix} C_{DD}^{F} + \dfrac{p_F D C_{LP}^{F}}{2V} \\ \dfrac{q D C_{MQ}^{F}}{2V} \\ \dfrac{r D C_{NR}^{F}}{2V} \end{Bmatrix} \tag{10}$$

Air density is computed using the center of gravity position of the projectile in concert with the standard atmosphere [14].

3. Dual-Spin Projectile Linear Theory

The equations of motion listed previously are highly nonlinear and not amenable to a closed-form analytic solution. Linear theory for symmetric rigid projectiles introduces a

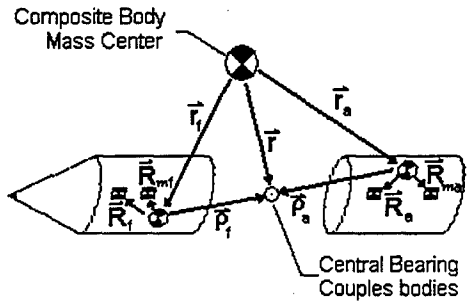

Figure 2. Dual-Spin Projectile Geometry.

sequence of assumptions, which yield a tractable set of linear differential equations of motion that can be solved in closed form. These equations form the basis of classic projectile stability theory. The same set of assumptions can be used to establish a linear theory for dual-spin projectiles in atmospheric flight.

A) Change of variables from fixed plane, station line velocity, u, to total velocity, V. Equations 11 and 12 relate V and u and their derivatives.

$$V = \sqrt{u^2 + v^2 + w^2} \tag{11}$$

$$\dot{V} = \frac{u\dot{u} + v\dot{v} + w\dot{w}}{V} \tag{12}$$

B) Change of variables from time, t, to dimensionless arc length, s. The dimensionless arc length, as defined by Murphy [15] is given in equation 13 and has units of calibers of travel.

$$s = \frac{1}{D} \cdot \int_0^t V \cdot d\tau \tag{13}$$

Equations 14 and 15 relate time and arc length derivatives of a given quantity ζ. Dotted terms refer to time derivatives, and primed terms denote arc length derivatives.

$$\dot{\zeta} = \left(\frac{V}{D}\right)\zeta' \tag{14}$$

$$\ddot{\zeta} = \left(\frac{V}{D}\right)^2 \left[\zeta'' + \frac{V'}{V}\zeta'\right] \tag{15}$$

C) Euler yaw and pitch angles are small so that

$$\sin(\theta) \approx \theta \qquad \cos(\theta) \approx 1$$

$$\sin(\psi) \approx \psi \qquad \cos(\psi) \approx 1 .$$

D) Aerodynamic angles of attack are small so that

$$\alpha \approx \frac{w}{V} \qquad \beta \approx \frac{v}{V} . \tag{16}$$

E) The projectile is mass balanced, such that the centers of gravity of both the forward and the aft bodies lie on the rotational axis of symmetry.

$$I_{XY}^A = I_{XY}^F = I_{XZ}^A = I_{XZ}^F = I_{YZ}^A = I_{YZ}^F = 0$$

$$I_{ZZ}^A = I_{YY}^A \qquad I_{ZZ}^F = I_{YY}^F$$

F) The projectile is aerodynamically symmetric such that

$$C_{MQ}^F = C_{NR}^F \qquad C_{MQ}^A = C_{NR}^A$$

$$C_{YO}^F = C_{YO}^A = C_{ZO}^F = C_{ZO}^A = 0$$

$$C_{YB1}^F = C_{ZB1}^F = C_{NA}^F$$

$$C_{YB1}^A = C_{ZB1}^A = C_{NA}^A$$

$$C_{NA} = C_{NA}^{F} + C_{NA}^{A} \qquad C_{MQ} = C_{MQ}^{F} + C_{MQ}^{A}$$

$$C_{XO} = C_{XO}^{F} + C_{XO}^{A} \cdot$$

G) A flat fire trajectory assumption is invoked, and the force of gravity is neglected.

H) The quantities V, ϕ_F, and ϕ_A are large compared to θ, ψ, q, r, v, and w, such that products of small quantities and their derivatives are negligible.

Application of the above assumptions results in equations 17–30.

$$x' = D \tag{17}$$

$$y' = \frac{D}{V} v + \psi D \tag{18}$$

$$z' = \frac{D}{V} w - \theta D \tag{19}$$

$$\phi_F' = \frac{D}{V} p_F \tag{20}$$

$$\phi_A' = \frac{D}{V} p_A \tag{21}$$

$$\theta' = \frac{D}{V} q \tag{22}$$

$$\psi' = \frac{D}{V} r \tag{23}$$

$$V' = -\left[\frac{\rho SD}{2m}\right](C_{XO})V \tag{24}$$

$$v' = -\left[\frac{\rho SD}{2m}\right]\left[(C_{NA})v - \left(\frac{D}{V}\right)\left(\frac{C^F_{NPA}}{2}p_F + \frac{C^A_{NPA}}{2}p_A\right)w\right] - Dr \tag{25}$$

$$w' = -\left[\frac{\rho SD}{2m}\right]\left[(C_{NA})w + \left(\frac{D}{V}\right)\left(\frac{C^F_{NPA}}{2}p_F + \frac{C^A_{NPA}}{2}p_A\right)v\right] + Dq \tag{26}$$

$$p'_F = \left[\frac{mD^2}{I^F_{XX}}\right]\left[\frac{\rho SD}{2m}\right]\left[\left(\frac{V}{D}\right)C^F_{DD} + \frac{C^F_{LP}}{2}p_F - \left(\frac{V}{D}\right)\left[\frac{C_{RB}\,sign(p_F - p_A)}{mD}\right]\left|m_F C^A_{XO} - m_A C^F_{XO}\right|\right] + C_V\left(\frac{D}{V}\right)\frac{(p_A - p_F)}{I^F_{XX}} \tag{27}$$

$$p'_A = \left[\frac{mD^2}{I^A_{XX}}\right]\left[\frac{\rho SD}{2m}\right]\left[\left(\frac{V}{D}\right)C^A_{DD} + \frac{C^A_{LP}}{2}p_A + \left(\frac{V}{D}\right)\left[\frac{C_{RB}\,sign(p_F - p_A)}{mD}\right]\left|m_F C^A_{XO} - m_A C^F_{XO}\right|\right] + C_V\left(\frac{D}{V}\right)\frac{(p_F - p_A)}{I^A_{XX}} \tag{28}$$

$$q' = \left[\frac{\rho SD}{2m}\right]\left[\frac{mD}{I^T_{YY}}\right]\left[\left(\frac{1}{V}\right)\left((Rm_{fx} + r_{fx})\frac{C^F_{NPA}}{2}p_F + (Rm_{ax} + r_{ax})\frac{C^A_{NPA}}{2}p_A\right)v + \frac{D}{2}(C_{MQ})q\right] + \left[\frac{\rho SD}{2m}\right]\left[\frac{mD}{I^T_{YY}}\right]\left[\left(\frac{1}{D}\right)\left((R_{fx} + r_{fx})C^F_{NA} + (R_{ax} + r_{ax})C^A_{NA}\right)w\right] - \frac{D}{V}\frac{(I^F_{XX}p_F + I^A_{XX}p_A)}{I^T_{YY}}r \tag{29}$$

$$r' = \left[\frac{\rho SD}{2m}\right]\left[\frac{mD}{I^T_{YY}}\right]\left[\left(\frac{1}{V}\right)\left((Rm_{fx} + r_{fx})\frac{C^F_{NPA}}{2}p_F + (Rm_{ax} + r_{ax})\frac{C^A_{NPA}}{2}p_A\right)w + \frac{D}{2}(C_{MQ})r\right] - \left[\frac{\rho SD}{2m}\right]\left[\frac{mD}{I^T_{YY}}\right]\left[\left(\frac{1}{D}\right)\left((R_{fx} + r_{fx})C^F_{NA} + (R_{ax} + r_{ax})C^A_{NA}\right)v\right] + \frac{D}{V}\frac{(I^F_{XX}p_F + I^A_{XX}p_A)}{I^T_{YY}}q \tag{30}$$

Equations 17–30 are linear, except for the total velocity, V, which is retained in several of the equations. Using the assumption that V changes very slowly with respect to the other variables, it is considered to be constant when it appears as a coefficient. With this assumption, the total velocity, the angle of attack dynamics, and the roll dynamics all become uncoupled, linear-time invariant equations of motion. The Magnus force in equations 25 and 26 is typically regarded as small in comparison to the other aerodynamic forces and is shown only for completeness. In further manipulation of the equations, all Magnus forces will be dropped. Magnus moments will

be retained, however, due to the magnitude amplification resulting from the cross product between Magnus force and its respective moment arm.

4. Epicyclic Modes of Oscillation

Equations 17–23 state that the fixed plane is mapped directly onto the inertial reference frame for the given assumptions. Equations 27 and 28 show that a roller bearing model requires knowledge of the zero-yaw drag on the forward and aft body separately. Also notice that the Magnus moments appear separately in equations 29 and 30. The equations for total velocity and the fore and aft spin rates have become completely decoupled from the angle of attack dynamics. It is a useful result to begin by studying equation 24, which represents the total velocity, V, of the projectile. Equation 24 is separable, and it is elementary to obtain the solution as downrange exponential decay.

$$V(s) = V_o e^{-\left(\frac{\rho SD}{2m} Cxo\right)s} \tag{31}$$

After extracting the decoupled equations for total velocity and fore and aft spin rates, there are only four equations remaining to examine. These equations describe fixed plane expressions for translational and rotational velocities v, w, q, and r. The angle of attack dynamics are driven directly by these four equations because the aerodynamic angles of attack depend on v and w by definition.

Using equation 31 and the definition for small angles of attack given in equation 16, the following two relations can be written.

$$\alpha(s) = \frac{w(s)}{V(s)} = \frac{w(s)}{V_o} e^{\left(\frac{\rho SD}{2m} Cxo\right)s} \tag{32}$$

$$\beta(s) = \frac{v(s)}{V(s)} = \frac{v(s)}{V_o} e^{\left(\frac{\rho SD}{2m} Cxo\right)s} \tag{33}$$

The translational and rotation velocities are described in a compact form as shown in equation 34,

$$\begin{Bmatrix} v' \\ w' \\ q' \\ r' \end{Bmatrix} = \begin{bmatrix} -A & 0 & 0 & -D \\ 0 & -A & D & 0 \\ \frac{B}{D} & \frac{C}{D} & E & -F \\ \frac{-C}{D} & \frac{B}{D} & F & E \end{bmatrix} \begin{Bmatrix} v \\ w \\ q \\ r \end{Bmatrix}. \tag{34}$$

where

$$A = \left[\frac{\rho SD}{2m}\right](C_{NA}) \tag{35}$$

$$B = \left[\frac{\rho SD}{2m}\right]\left[\frac{mD}{I_{YY}^T}\right]\left(\frac{D}{V}\right)\left((Rm_{fx} + r_{fx})\frac{C_{NPA}^F}{2} p_F + (Rm_{ax} + r_{ax})\frac{C_{NPA}^A}{2} p_A\right) \tag{36}$$

$$C = \left[\frac{\rho SD}{2m}\right]\left[\frac{mD}{I_{YY}^T}\right] C_{MA} \tag{37}$$

$$E = \left[\frac{\rho SD}{2m}\right]\left[\frac{mD^2}{I_{YY}^T}\right]\frac{C_{MQ}}{2} \tag{38}$$

$$F = \frac{D}{V}\frac{(I_{XX}^F p_F + I_{XX}^A p_A)}{I_{YY}^T} \tag{39}$$

$$C_{MA} = \left((R_{fx} + r_{fx})C_{NA}^F + (R_{ax} + r_{ax})C_{NA}^A\right) \tag{40}$$

$$I_{YY}^T = I_{YY}^F + m_f r_{fx}^2 + I_{YY}^A + m_a r_{ax}^2. \tag{41}$$

Eigenvalues of equation 34 provide the fast and slow epicyclic modes of oscillation for v, w, q, and r. The four roots of the characteristic equation are displayed below.

$$s=\begin{Bmatrix}\frac{1}{2}\cdot\left[(E-A)+iF\pm\sqrt{(E-A)^2-F^2+4(AE+C)+2iF\left(E-A+\frac{2(AF+B)}{F}\right)}\right]\\ \frac{1}{2}\cdot\left[(E-A)-iF\pm\sqrt{(E-A)^2-F^2+4(AE+C)-2iF\left(E-A+\frac{2(AF+B)}{F}\right)}\right]\end{Bmatrix}=\begin{Bmatrix}\lambda_F+i\Phi_F\\ \lambda_S+i\Phi_S\\ \lambda_F-i\Phi_F\\ \lambda_S-i\Phi_S\end{Bmatrix} \quad (42)$$

Linear combinations of the previous equations lead to equation 43.

$$\begin{bmatrix}(E-A)\\ iF\\ -AE-C\\ -i(AF+B)\end{bmatrix}=\begin{bmatrix}\lambda_F+\lambda_S\\ i(\Phi_F+\Phi_S)\\ \lambda_F\lambda_S-\Phi_F\Phi_S\\ i(\lambda_F\Phi_S+\lambda_S\Phi_F)\end{bmatrix} \quad (43)$$

In line with rigid body, six degrees of freedom projectile stability analysis, two more simplifications based on size are introduced. First, neglect the product of the damping factors compared to the product of the damped natural frequencies. Secondly, neglect the product of A and E, because multiples of the relative density factor are small compared with the magnitudes of other terms. A solution may now be obtained for both the fast and the slow damping factors and turning rates for the translational and rotational velocities.

$$\lambda_F=\frac{-(A-E)}{2}\left[1+\frac{F}{\sqrt{F^2-4C}}\left(1-\frac{(2AF+2B)}{F(A-E)}\right)\right] \quad (44)$$

$$\Phi_F=\frac{1}{2}\left[F+\sqrt{F^2-4C}\right] \quad (45)$$

$$\lambda_S = \frac{-(A-E)}{2}\left[1-\frac{F}{\sqrt{F^2-4C}}\left(1-\frac{(2AF+2B)}{F(A-E)}\right)\right] \tag{46}$$

$$\Phi_S = \frac{1}{2}\left[F-\sqrt{F^2-4C}\right] \tag{47}$$

Before making conclusions about the stability of the angle of attack dynamics, the damping factors and the damped natural frequencies have to be calculated for α and β rather than v and w. These new damping factors will account for the fact that v, w, and V all decay downrange. Whether α and β are stable depends on which quantities decay fastest. Two new damping factors are introduced based on equations 32 and 33.

$$\lambda_F^* = \frac{-\left(A-2\frac{\rho SD}{2m}C_{XO}-E\right)}{2}\left[1+\frac{F}{\sqrt{F^2-4C}}\left(1-\frac{\left(2AF+2\frac{\rho SD}{2m}C_{XO}F+2B\right)}{F\left(A-2\frac{\rho SD}{2m}C_{XO}-E\right)}\right)\right] \tag{48}$$

$$\lambda_S^* = \frac{-\left(A-2\frac{\rho SD}{2m}C_{XO}-E\right)}{2}\left[1-\frac{F}{\sqrt{F^2-4C}}\left(1-\frac{\left(2AF+2\frac{\rho SD}{2m}C_{XO}F+2B\right)}{F\left(A-2\frac{\rho SD}{2m}C_{XO}-E\right)}\right)\right] \tag{49}$$

The fast and slow turning rates represent the imaginary parts of the complex eigenvalues. These will remain unchanged for α and β, because division by V(s) in equations 32 and 33 only affects the real parts of the eigenvalues. If either Φ_F or Φ_S is complex, there will be a positive real part in one of the four eigenvalues. To avoid complex turning rates, the term under the radical in equations 45 and 47 must be greater than zero, introducing the idea of the gyroscopic stability factor S_G.

$$S_G \equiv \frac{F^2}{4 \cdot C} > 1 \tag{50}$$

Furthermore, the dynamic stability factor is defined by equation 51.

$$S_D = \frac{\left(2AF + 2\frac{\rho SD}{2m} C_{XO} F + 2B\right)}{F\left(A - 2\frac{\rho SD}{2m} C_{XO} - E\right)} \tag{51}$$

The fast mode damping factor, λ_F^*, must be negative for stable flight. To ensure stability, the following two conditions must be satisfied.

$$\left(A - 2\frac{\rho SD}{2m} C_{XO} - E\right) > 0 \tag{52}$$

$$\frac{1}{S_G} < S_D(2 - S_D) \tag{53}$$

The results shown in equations 50–53 are very similar to conventional rigid body projectile analysis. Hence, dual-spin projectile stability analysis can be approached in essentially the same manner that rigid projectiles are analyzed. Differences in stability characteristics arise from the coefficients F and B. The coefficient F contains terms with forward and aft body roll rate and roll inertia appearing separately. Magnus moments also appear separated in the coefficient B, due to their dependence on the fore and aft roll rates.

5. Dual-Spin Projectile Stability

The gyroscopic and dynamic stability factors can be reexpressed as shown in equations 54 and 55.

$$S_G = \frac{(I_{XX}^T \tilde{p})^2}{2 I_{YY}^T M} \tag{54}$$

$$S_D = \frac{2(C_{NA} - C_{XO}) + G^T p^*}{(C_{NA} - 2C_{XO}) - \left[\frac{mD^2}{I_{YY}^T}\right]\frac{(C_{MQ})}{2}}, \tag{55}$$

where

$$\tilde{p} = \frac{(p_F + \gamma_{DS}\, p_A)}{(1 + \gamma_{DS})} \tag{56}$$

$$\gamma_{DS} = \frac{I_{XX}^A}{I_{XX}^F} \tag{57}$$

$$I_{XX}^T = (I_{XX}^F + I_{XX}^A) = I_{XX}^F (1 + \gamma_{DS}) \tag{58}$$

$$M = \rho S V^2 C_{MA} \tag{59}$$

$$p^* = \frac{(p_F + \mu_{DS}\, p_A)}{(1 + \mu_{DS})} \tag{60}$$

$$\mu_{DS} = \frac{(Rm_{ax} + r_{ax})C_{NPA}^A}{(Rm_{fx} + r_{fx})C_{NPA}^F} \tag{61}$$

$$G^T = \frac{mD}{I_{yy}^T}\left(\frac{D}{V}\right)\left((Rm_{fx} + r_{fx})C_{NPA}^F\right)(1 + \mu_{DS}). \tag{62}$$

The inertia weighted average spin rate for the composite body, $\tilde{p}$, is biased to the spin rate of the body with the largest roll inertia component. The Magnus weighted average spin rate, p^*, behaves in precisely the same manner as $\tilde{p}$; however, it is biased toward the body with the largest Magnus moment. A plot of $\tilde{p}$ vs. roll inertia ratio, γ_{DS}, and p^* vs. Magnus ratio,

μ_{DS}, is shown in Figure 3. When $\gamma_{DS} = 0$, $\tilde{p}$ is equal to p_F, while as $\gamma_{DS} \to \infty$, $\tilde{p}$ approaches p_A. Similar relations hold between μ_{DS} and p^*. Gyroscopic stability factor vs. inertia weighted average spin rate is plotted as Figure 4 for various values of composite inertia and external moments.

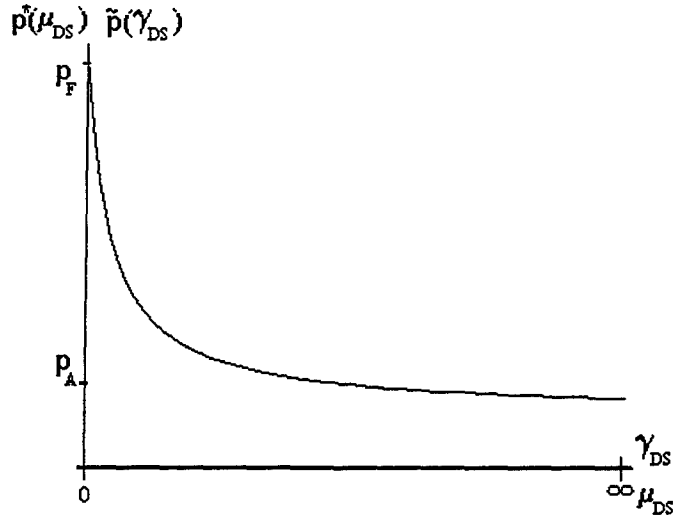

Figure 3. Inertia Weighted Average Spin Rate vs. Roll Inertia Ratio.

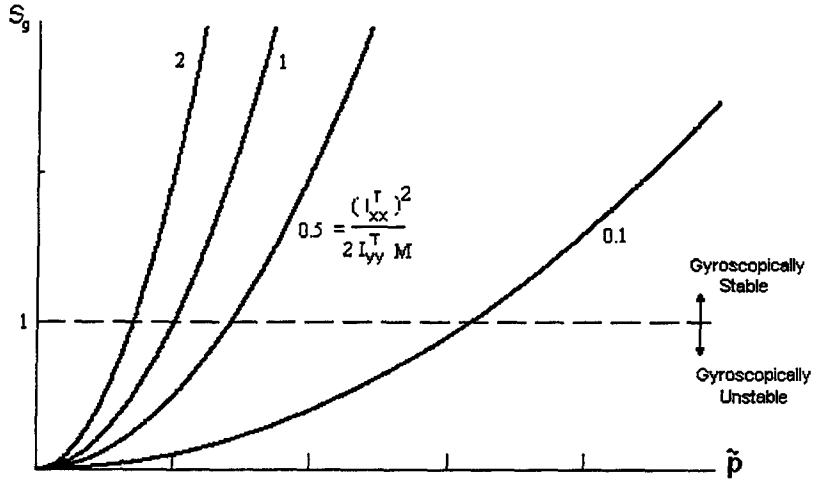

Figure 4. Gyroscopic Stability Factor, S_G, vs. Inertia Weighted Average Spin Rate.

It is interesting to expand equation 55 and examine the results. The dynamic stability factor can be broken into two parts. The first part, shown in equation 64 represents a stability factor offset that is independent of whether the system is a rigid or dual-spin projectile. Equation 65 shows the second part, which does vary with respect to the rigid projectile case depending on the Magnus moment coefficients and spin rates. This portion of the total stability factor is directly proportional to the total Magnus moment acting about the composite center of mass and can be considered as a dynamic stability enhancement factor.

$$S_D = H + \Delta_{DS} \ , \tag{63}$$

where

$$H = \left(\frac{2\left(C_{NA} - C_{XO}\right)}{\left(C_{NA} - 2C_{XO}\right) - \left[\frac{mD^2}{I_{YY}^T}\right]\frac{\left(C_{MQ}\right)}{2}} \right) \tag{64}$$

$$\Delta_{DS} = \left(\frac{G^T p^*}{\left(C_{NA} - 2C_{XO}\right) - \left[\frac{mD^2}{I_{YY}^T}\right]\frac{\left(C_{MQ}\right)}{2}} \right) . \tag{65}$$

It is also informative to compare the dual-spin projectile stability factors to the conventional rigid projectile results. To do this, define $\overline{p}$ and Δp as the average spin rate and the spin rate difference, respectively. Thus,

$$p_F = \overline{p} + \Delta p \qquad p_A = \overline{p} - \Delta p \ .$$

The spin rate of an equivalent rigid projectile is $\overline{p}$. The ratio of the dual-spin gyroscopic stability factor to the rigid projectile gyroscopic stability factor is shown as equation 66.

Equation 67 shows the ratio of dynamic stability enhancement factors between the dual-spin case and the rigid projectile case. These two relations are again of very similar form.

$$\frac{S_{G_{DS}}}{S_G} = \left(1 + \frac{1-\gamma_{DS}}{1+\gamma_{DS}} \frac{\Delta p}{\bar{p}}\right)^2 \tag{66}$$

$$\frac{\Delta_{DS}}{\Delta} = \left(1 + \frac{1-\mu_{DS}}{1+\mu_{DS}} \frac{\Delta p}{\bar{p}}\right) \tag{67}$$

Figures 5 and 6 represent equation 66 as a function of the roll inertia ratio and the differential spin ratio. When the gyroscopic stability factor ratio is greater than one, dual-spin gyroscopic stability is enhanced compared to the rigid projectile with a roll rate of $\bar{p}$. It can be shown that the differential spin ratio is positive when the forward body is spinning faster than the aft, and negative when the reverse is true. The curves can also be grouped by the roll inertia ratio. When γ_{DS} is less than one, the forward body has more roll inertia. The aft inertia is larger when γ_{DS} is greater than one. Based on the values of the differential spin ratio and roll inertia ratio, Figures 5 and 6 can be viewed in separate quadrants. When both ratios favor one of the bodies, gyroscopic stability is enhanced. When the ratios favor opposite bodies, the stability factor is diminished. Note that the gyroscopic stability ratio can never become negative because the values compared are squared. Also note that in physical systems, the differential spin ratio must be zero when γ_{DS} goes to zero or infinity.

Figures 7 and 8 represent equation 66 as a function of the Magnus ratio and the differential spin ratio. When the magnitude of the dynamic enhancement ratio is greater than one, both the total Magnus moment and the dynamic stability enhancement factor are larger than the rigid projectile case. This can result from several physical situations, which are represented by again considering the graphs in sections.

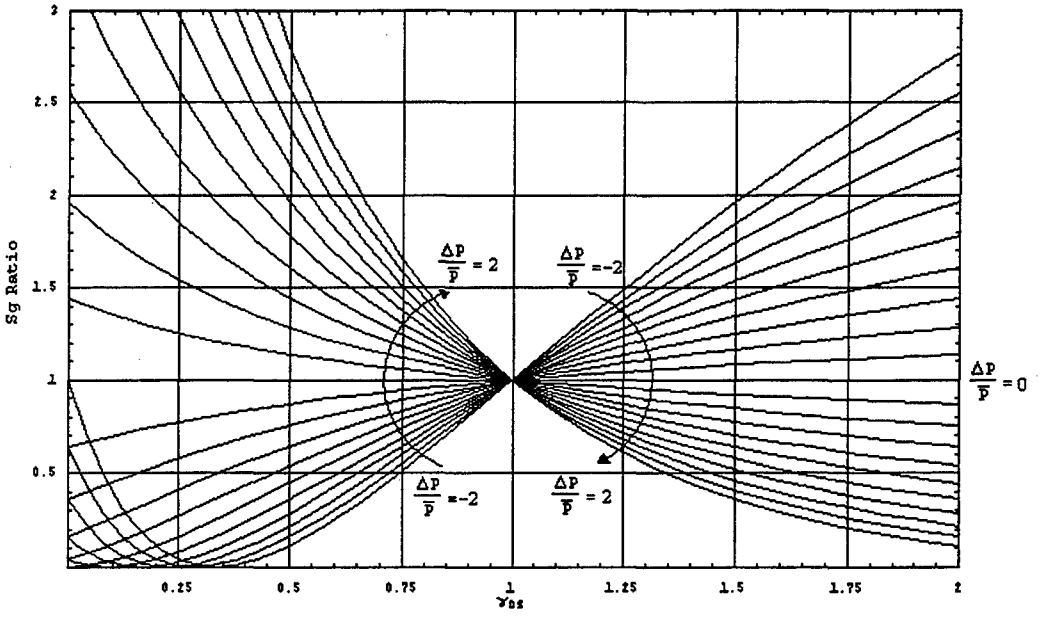

Figure 5. Gyroscopic Spin Ratio vs. Gamma Dual Spin.

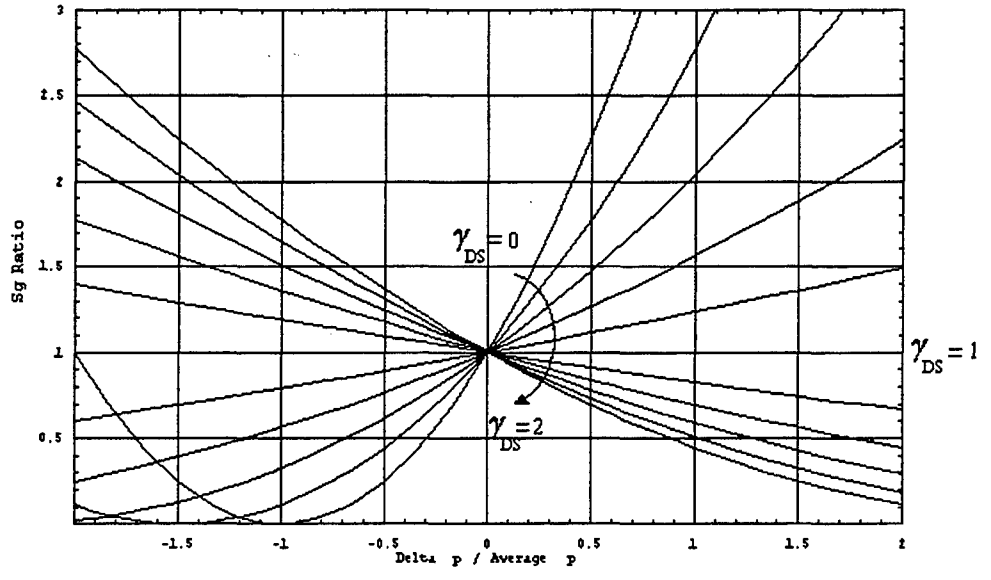

Figure 6. Gyroscopic Stability Ratio vs. Differential Spin Ratio.

When the Magnus ratio is between negative and positive one, the Magnus moment coefficient is larger for the forward body than for the aft. When the Magnus ratio is outside of

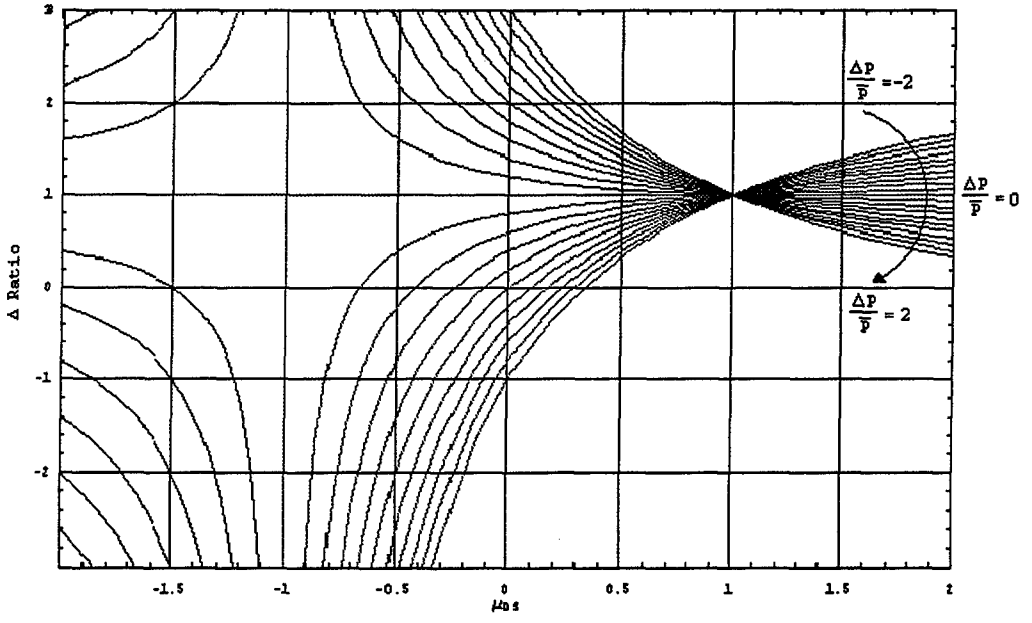

Figure 7. Delta Ratio vs. Magnus Ratio.

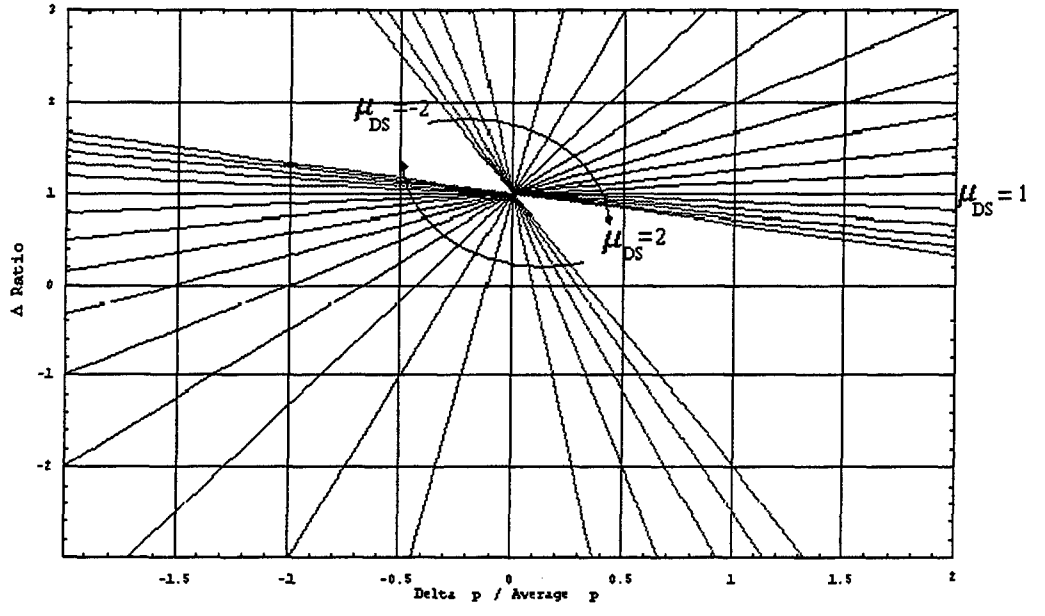

Figure 8. Delta Ratio vs. Differential Spin Ratio.

these boundaries, the aft body has a larger Magnus coefficient. Negative Magnus ratios indicate that the aft Magnus center of pressure is rearward of the composite body mass center. Positive

values of the differential spin ratio again indicate that the forward body is spinning faster than the aft. With this in mind, Figures 7 and 8 can be viewed where both ratios favor one body, or where they favor opposite bodies. For the first case, the total Magnus moment applied to the dual-spin projectile is larger than that of the rigid case. The opposite is true when the ratios favor opposite bodies.

Some special values of Magnus ratio must also be considered. Magnus ratio equal to one indicates the Magnus coefficients are equivalent or, physically, that the centers of pressure and force coefficients are equivalent. In this situation, the dual-spin case will have the same Magnus moment as the rigid case because p^* and $\overline{p}$ do not differ. When Magnus ratio is equal to negative one, the Magnus coefficients are equal and opposite. For the rigid case where the bodies spin together, the Magnus moment will go to zero and drive the enhancement ratio to infinity.

Dual-spin projectile stability results must match the standard rigid projectile stability results in two situations. First, either of the bodies may be neglected by setting their mass and inertia properties and force coefficients to zero. In this case, the inertia properties of the total body reduce to those of the remaining body and the roll inertia ratio becomes either 0 or ∞, depending on which body remains. Using the same logic, $\overline{p}$ becomes either p_F or p_A. Also, the moments considered, including Magnus, are only those applied to the remaining body. With these assumptions, the rigid body stability results are obtained.

The second case to consider is when the forward and aft bodies spin together. For this case, both the inertia weighted average spin rate and the Magnus weighted average spin rate are equal to both the front and rear spin rates, since the projectile bodies are spinning together. This result is true regardless of the roll inertia ratio. The inertia properties are for the total body, as are the applied moments. Again, the rigid body stability results are obtained.

6. Epicyclic Pitching and Yawing Motion

Equation 34 has been used to solve for the dynamic modes of projectile pitching and yawing motion along its flight path. To complete the analytical solution, the two complex conjugate pairs of modes in equation 41 must be used to evaluate the system mode shapes. Solutions will be obtained for v and w, and these will be used to evaluate α and β .

Mode shapes for equation 34 are displayed in the matrix V, described by equations 68–72 using the familiar coefficients. By applying the relations in equation 43, equations 68–72 can be expressed completely in terms of the coefficient A, and the fast and slow mode damping factors and turning rates.

$$[V]=\begin{bmatrix} i & i & -i & -i \\ 1 & 1 & 1 & 1 \\ \frac{K+\sqrt{Q}}{2D} & \frac{K-\sqrt{Q}}{2D} & \frac{R+\sqrt{S}}{2D} & \frac{R-\sqrt{S}}{2D} \\ -\frac{i(K+\sqrt{Q})}{2D} & -\frac{i(K-\sqrt{Q})}{2D} & \frac{i(R+\sqrt{S})}{2D} & \frac{i(R-\sqrt{S})}{2D} \end{bmatrix}, \tag{68}$$

where

$$K=(E-A)+2A+iF=(\lambda_F+\lambda_S)+2A+i(\Phi_F+\Phi_S) \tag{69}$$

$$Q=(E-A)^2+4AE+4C-F^2+2i\big(F(E-A)+2(AF+B)\big)=\big((\lambda_F-\lambda_S)+i(\Phi_F-\Phi_S)\big)^2 \tag{70}$$

$$R=(E-A)+2A-iF=(\lambda_F+\lambda_S)+2A-i(\Phi_F+\Phi_S) \tag{71}$$

$$S=(E-A)^2+4AE+4C-F^2-2i\big(F(E-A)+2(AF+B)\big)=\big((\lambda_F-\lambda_S)-i(\Phi_F-\Phi_S)\big)^2. \tag{72}$$

Recognizing that the turning rates are between one and two orders of magnitude greater than the damping factors, equation 68 can be simplified to equation 73.

$$[V]=\begin{bmatrix} i & i & -i & -i \\ 1 & 1 & 1 & 1 \\ i\dfrac{\Phi_F - iA}{D} & i\dfrac{\Phi_S - iA}{D} & -i\dfrac{\Phi_F + iA}{D} & -i\dfrac{\Phi_S + iA}{D} \\ \dfrac{\Phi_F - iA}{D} & \dfrac{\Phi_S - iA}{D} & \dfrac{\Phi_F + iA}{D} & \dfrac{\Phi_S + iA}{D} \end{bmatrix} \tag{73}$$

Once these simplified mode shapes are obtained, the initial conditions for v, w, q, and r can be used to complete the solution. Equations 74 and 75 are the analytical solutions for the fixed plane translational velocities v and w, expressed in phase-amplitude form.

$$v(s) = V_1 e^{\lambda_F s} \sin(\Phi_F s + \Theta_{V1}) + V_2 e^{\lambda_S s} \sin(\Phi_S s + \Theta_{V2}) \tag{74}$$

$$w(s) = V_1 e^{\lambda_F s} \sin(\Phi_F s + \Theta_{w1}) + V_2 e^{\lambda_S s} \sin(\Phi_S s + \Theta_{w2}), \tag{75}$$

where

$$V_1 = \sqrt{\frac{(w_o' - v_o\Phi_S)^2}{(\Phi_F - \Phi_S)^2} + \frac{(-v_o' - w_o\Phi_S)^2}{(\Phi_F - \Phi_S)^2}} \qquad \Theta_{V1} = \tan^{-1}\left(\frac{w_o' - v_o\Phi_S}{-(-v_o' - w_o\Phi_S)}\right) \tag{76}$$

$$V_2 = \sqrt{\frac{(w_o' - v_o\Phi_F)^2}{(\Phi_F - \Phi_S)^2} + \frac{(-v_o' - w_o\Phi_F)^2}{(\Phi_F - \Phi_S)^2}} \qquad \Theta_{V2} = \tan^{-1}\left(\frac{-(w_o' - v_o\Phi_F)}{-v_o' - w_o\Phi_F}\right) \tag{77}$$

$$\Theta_{W1} = \tan^{-1}\left(\frac{-v_o' - w_o\Phi_S}{w_o' - v_o\Phi_S}\right) \tag{78}$$

$$\Theta_{W2} = \tan^{-1}\left(\frac{-(-v_o' - w_o\Phi_F)}{-(w_o' - v_o\Phi_F)}\right). \tag{79}$$

7. Dual-Spin Projectile Swerve

Having established the conditions for stability and analytically solving for the translational motion of v and w, it is now possible to solve for the swerving motion of the projectile as it travels downrange. Swerving motion is defined as projectile motion measured along the earth-fixed Y and Z-axes. To an observer standing behind the gun tube, these axes are oriented such that positive Y is to the right and positive Z is pointed downward. The swerving motion is a result of the normal aerodynamic forces exerted on the projectile during its flight, as it pitches and yaws due to the angle of attack dynamics.

By differentiating the $\vec{j}_n$ and $\vec{k}_n$ components of equation 1 with respect to time, and substituting in the proper components of equation 3, equations 80 and 81 are generated.

$$\ddot{y} = \left[\frac{\rho SD}{2m}\right]\left(\frac{V}{D}\right)\left(-C_{XO}V\psi - C_{NA}v\right) \tag{80}$$

$$\ddot{z} = \left[\frac{\rho SD}{2m}\right]\left(\frac{V}{D}\right)\left(C_{XO}V\theta - C_{NA}w\right) \tag{81}$$

Equations 80 and 81 are second-order differential equations with respect to time. Rewriting these differential equations with respect to dimensionless arc length results in the final form of the equations governing the swerve dynamics. Dividing through by the characteristic length of the projectile gives results for dimensionless swerve, measured in calibers of travel.

$$\left(\frac{y}{D}\right)'' = \left[\frac{\rho SD}{2m}\right]\left(C_{XO} - C_{NA}\right)\left(\frac{v}{V}\right) \tag{82}$$

$$\left(\frac{z}{D}\right)'' = \left[\frac{\rho SD}{2m}\right]\left(C_{XO} - C_{NA}\right)\left(\frac{w}{V}\right) \tag{83}$$

Consideration of equations 31, 72, and 73 lead to a double integration, which yields the solution for downrange swerve. This solution does account for the exponential change in V, and all the derived conditions of stability apply. Upon integrating, recognize that the damping factors λ_F^* and λ_S^* are small compared to the turning rates and will be neglected in the amplitudes, phase angles, and integration constants.

The final results after integration are displayed as equations 84 and 85.

$$\frac{y(s)}{D} = \frac{y_o}{D} + \left(\psi_o + \frac{v_o}{V_o}\right)s + \left[\frac{\rho SD}{2m}\right]\frac{(C_{XO} - C_{NA})}{V_o}\left(\frac{V_1}{\Phi_F^2}\left(\exp(\lambda_F^* s)\sin(\Phi_F s + \Theta_{V1} - \pi) - \sin(\Theta_{V1} - \pi) - \Phi_F \cos(\Theta_{V1} - \pi)s\right)\right) + \left[\frac{\rho SD}{2m}\right]\frac{(C_{XO} - C_{NA})}{V_o}\left(+\frac{V_2}{\Phi_S^2}\left(\exp(\lambda_S^* s)\sin(\Phi_S s + \Theta_{V2} - \pi) - \sin(\Theta_{V2} - \pi) - \Phi_S \cos(\Theta_{V2} - \pi)s\right)\right) \quad (84)$$

$$\frac{z(s)}{D} = \frac{z_o}{D} + \left(-\theta_o + \frac{w_o}{V_o}\right)s + \left[\frac{\rho SD}{2m}\right]\frac{(C_{XO} - C_{NA})}{V_o}\left(\frac{V_1}{\Phi_F^2}\left(\exp(\lambda_F^* s)\sin(\Phi_F s + \Theta_{W1} - \pi) - \sin(\Theta_{W1} - \pi) - \Phi_F \cos(\Theta_{W1} - \pi)s\right)\right) + \left[\frac{\rho SD}{2m}\right]\frac{(C_{XO} - C_{NA})}{V_o}\left(+\frac{V_2}{\Phi_S^2}\left(\exp(\lambda_S^* s)\sin(\Phi_S s + \Theta_{W2} - \pi) - \sin(\Theta_{W2} - \pi) - \Phi_S \cos(\Theta_{W2} - \pi)s\right)\right) \quad (85)$$

These equations for swerve include terms representing the point mass trajectory, the epicyclic swerving motion and a new term called "jump." Both jump terms, J_Y and J_Z, are summarized below.

$$J_Y = -\left[\frac{\rho SD}{2m}\right]\frac{(C_{XO} - C_{NA})}{V_o}\left(\frac{V_1}{\Phi_F}\cos(\Theta_{V1} - \pi) + \frac{V_2}{\Phi_S}\cos(\Theta_{V2} - \pi)\right)s = \left[\frac{\rho SD}{2m}\right]\frac{(C_{XO} - C_{NA})}{V_o}\left(\frac{v_o' + w_o(\Phi_F + \Phi_S)}{\Phi_F \Phi_S}\right)s \quad (86)$$

$$J_Z = -\left[\frac{\rho SD}{2m}\right]\frac{(C_{XO}-C_{NA})}{V_o}\left(\frac{V_1}{\Phi_F}\cos(\Theta_{W1}-\pi)+\frac{V_2}{\Phi_S}\cos(\Theta_{W2}-\pi)\right)s$$
$$= \left[\frac{\rho SD}{2m}\right]\frac{(C_{XO}-C_{NA})}{V_o}\left(\frac{w_o' - v_o(\Phi_F+\Phi_S)}{\Phi_F\Phi_S}\right)s \tag{87}$$

Recalling the relations in equation 43, the jump terms can finally be rewritten as equations 88 and 89.

$$J_Y = \frac{(C_{XO}-C_{NA})}{\frac{mD}{I_{yy}^T}C_{MA}}\left(\frac{v_o'}{V_o}+\frac{w_o}{V_o}\left(\frac{D}{V}\right)\left(\frac{I_{XX}^T}{I_{YY}^T}\right)\tilde{p}\right)s \tag{88}$$

$$J_Z = \frac{(C_{XO}-C_{NA})}{\frac{mD}{I_{yy}^T}C_{MA}}\left(\frac{w_o'}{V_o}-\frac{v_o}{V_o}\left(\frac{D}{V}\right)\left(\frac{I_{XX}^T}{I_{YY}^T}\right)\tilde{p}\right)s \tag{89}$$

Jump results from the initial pitching and yawing conditions and is introduced into the swerve equations after the first integration. Jump has been shown to have a much more significant effect on the final trajectory than epicyclic swerve. These expressions for jump show the similarities with the rigid projectile case. The only difference is the use of inertia weighted average spin rate.

8. Conclusions

The equations of motion for a dual-spin projectile in atmospheric flight have been developed. The model allows for unbalanced forward and aft components. The bearing that connects the forward and aft components is a combination hydrodynamic and roller bearing.

After appropriate simplifications are made to the initial nonlinear equations, it is shown that the roller bearing requires knowledge of the axial force on each projectile body in the determination of the roll dynamics. This fact will require range reduction algorithms to be

modified to estimate the axial force on both components from roll angle and roll data. The hydrodynamic bearing does not have this complication because the reaction moment on a hydrodynamic bearing is a function of the roll rate difference only.

It is possible to analyze the stability of a dual-spin projectile using a methodology similar to rigid body projectile stability analysis. The gyroscopic stability factor, S_G, is different from the conventional rigid projectile results. It depends on the spin rates of both bodies as well as their individual roll inertias. However, it is possible to define the inertia weighted average spin rate, $\tilde{p}$, which is essentially an equivalent spin rate such that the form of the gyroscopic stability factor is the same as the rigid projectile case. When either the fore or aft body is removed, or both bodies spin together, the stability results reduce to the standard rigid projectile stability results.

The dynamic stability factor is also different from the conventional rigid projectile results. To emulate the standard results, a Magnus weighted average spin rate, p^* is introduced. The dynamic stability factor can be shown to match the rigid case under the same two conditions that were checked for the gyroscopic stability factor. The dynamic stability enhancement ratio depends on the differential spin ratio and the Magnus ratio, which may both become negative.

INTENTIONALLY LEFT BLANK.

9. References

1. Likins, P. W. "Attitude Stability Criteria for Dual-Spin Spacecraft." *Journal of Spacecraft and Rockets*, vol. 4, pp. 1638–1643, 1967.

2. Cloutier, G. J. "Stable Rotation States of Dual-Spin Spacecraft." *Journal of Spacecraft and Rockets,* vol. 5, pp. 490–492, 1968.

3. Mingori, D. L. "Effects of Energy Dissipation on the Attitude Stability of Dual Spin Satellites." *AIAA Journal*, vol. 7, pp. 20–27, 1969.

4. Fang, B. T. "Energy Considerations for Attitude Stability of Dual-Spin Spacecraft." *Journal of Spacecraft and Rockets*, vol. 5, pp. 1241–1243, 1968.

5. Hall, C. D., and R. H. Rand. "Spinup Dynamics of Axial Dual-Spin Spacecraft." *Journal of Guidance, Control, and Dynamics*, vol. 17, pp. 30–37, 1994.

6. Or, A. C. "Resonances in the Despin Dynamics of Dual-Spin Spacecraft." *Journal of Guidance, Control, and Dynamics*, vol. 14, pp. 321–329, 1991.

7. Cochran, J. E., P. H. Shu, and S. D. Rew. "Attitude Motion of Asymmetric Dual-Spin Spacecraft." *Journal of Guidance, Control, and Dynamics*, vol. 5, pp. 37–42, 1982.

8. Tsuchiya, K. "Attitude Behavior of a Dual-Spin Spacecraft Composed of Asymmetric Bodies." *Journal of Guidance, Control, and Dynamics*, vol. 2, pp. 328–333, 1979.

9. Yang, H. X. "Method for Stability Analysis of Asymmetric Dual-Spin Spacecraft." *Journal of Guidance, Control, and Dynamics*, vol. 12, pp. 123–125, 1989.

10. Viderman, Z., F. P. J. Rimrott, and W. L. Cleghorn. "Stability of an Asymmetric Dual-Spin Spacecraft with Flexible Platform." *Journal of Guidance, Control, and Dynamics*, vol. 14, pp. 751–760, 1991.

11. Stabb, M. C., and A. L. Schlack. "Pointing Accuracy of a Dual-Spin Satellite Due to Torsional Appendage Vibrations." *Journal of Guidance, Control, and Dynamics,* vol. 16, pp. 630–635, 1991.

12. Smith, J. A., K. A. Smith, and R. Topliffe. "Feasibility Study for Application of Modular Guidance and Control Units to Existing ICM Projectiles." Final Technical Report, Contractor Report ARLCD-CR-79001, U.S. Army Armament Research and Development Command, 1978.

13. Etkin, B. *Dynamics of Atmospheric Flight.* New York, NY: John Wiley and Sons, 1972.

14. Von Mises, R. *Theory of Flight.* New York, NY: Dover Publications Inc., 1959.

15. Murphy, C. H. "Free Flight Motion of Symmetric Missiles." BRL Report No. 1216, U.S. Army Ballistic Research Laboratories, Aberdeen Proving Ground, MD, 1963.

Appendix:

Rotation Dynamic Equations

INTENTIONALLY LEFT BLANK.

The rotation kinetic differential equations are derived by splitting the two-body system at the bearing connection point. A constraint force, $\vec{F}_C$, and a constraint moment, $\vec{M}_C$, couple the forward and aft bodies. The translational dynamic equations for both bodies are given by equations A-1 and A-2.

$$m_A \vec{a}_{A/I} = \vec{F}_A + \vec{F}_C \tag{A-1}$$

$$m_F \vec{a}_{F/I} = \vec{F}_F - \vec{F}_C \tag{A-2}$$

Key to the development of the rotation kinetic differential equations is the ability to solve for the constraint forces and moments as a function of state variables and time derivatives of state variables. An expression for the constraint force can be obtained by subtracting equation A-2 from equation A-1.

$$\frac{m}{m_F m_A}\vec{F}_C = \frac{\vec{F}_F}{m_F} - \frac{\vec{F}_A}{m_A} + \vec{a}_{A/I} - \vec{a}_{F/I} \tag{A-3}$$

With the constraint force known, the rotational dynamic equations for the forward and aft bodies can be developed. The constraint force contributes to the applied moments from a cross product between the constraint force vector and the position vectors from the individual centers of gravity to the bearing. An additional constraint moment couples the forward and aft bodies due to viscous or rolling friction in the bearing.

$$\frac{d}{dt}\vec{H}_{A/I} = \vec{M}_A + \vec{M}_V + \vec{\rho}_A \times \vec{F}_C \tag{A-4}$$

$$\frac{d}{dt}\vec{H}_{F/I} = \vec{M}_F - \vec{M}_V - \vec{\rho}_F \times \vec{F}_C \,, \tag{A-5}$$

where

$$\vec{\rho}_A = \vec{r}_A - \vec{r} \tag{A-6}$$

$$\vec{\rho}_F = \vec{r}_F - \vec{r} \ . \tag{A-7}$$

The acceleration of the mass center of the forward and aft bodies, $\vec{a}_{F/I}$ and $\vec{a}_{A/I}$, can be expressed in terms of the acceleration of the composite body mass center. After making this substitution, the constraint force components in the fixed plane reference frame can be expressed in the following manner.

$$\begin{Bmatrix} F_{CX} \\ F_{CY} \\ F_{CZ} \end{Bmatrix} = [F_F] \begin{Bmatrix} \dot{p}_F \\ \dot{q} \\ \dot{r} \end{Bmatrix} + [F_A] \begin{Bmatrix} \dot{p}_A \\ \dot{q} \\ \dot{r} \end{Bmatrix} + \{F_0\} \tag{A-8}$$

The constraint moment components in the fixed plane reference frame acting on the forward body about the forward body mass center, and resulting from the constraint force cross product can be written in the following manner.

$$\begin{Bmatrix} M_{FC_{FX}} \\ M_{FC_{FY}} \\ M_{FC_{FZ}} \end{Bmatrix} = [M_{FF}] \begin{Bmatrix} \dot{p}_F \\ \dot{q} \\ \dot{r} \end{Bmatrix} + [M_{FA}] \begin{Bmatrix} \dot{p}_A \\ \dot{q} \\ \dot{r} \end{Bmatrix} + \{M_{F0}\} \tag{A-9}$$

In a similar way, the components in the fixed plane reference frame of the moment of the constraint force acting on the aft body about the aft body mass center can be written as shown in equation A-10.

$$\begin{Bmatrix} M_{FC_{AX}} \\ M_{FC_{AY}} \\ M_{FC_{AZ}} \end{Bmatrix} = [M_{AF}] \begin{Bmatrix} \dot{p}_F \\ \dot{q} \\ \dot{r} \end{Bmatrix} + [M_{AA}] \begin{Bmatrix} \dot{p}_A \\ \dot{q} \\ \dot{r} \end{Bmatrix} + \{M_{A0}\} \tag{A-10}$$

The rotation kinetic differential equations are both expressed in the fixed plane reference frame. The equations are left general and allow for a fully populated inertia matrix and mass unbalance. Equations A-8–A-10 are substituted into both sets of rotation kinetic equations for the forward and aft bodies. At this point, both sets of equations still have unknown constraint moments at the bearing connection point. To eliminate the bearing constraint moments in the fixed plane $\vec{j}_n$ and $\vec{k}_n$ directions, the $\vec{j}_n$ and $\vec{k}_n$ components of the rotation kinetic equations for the forward and aft bodies are added together to form two dynamic equations that are free of constraint moments. In this way, the constraint moments at the bearing have been eliminated analytically from the pitching and yaw dynamics.

To finish expressing the roll dynamic equations, however, an expression for the unknown constraint moment must be formed. The moment transmitted across the bearing is modeled as a combination hydrodynamic and roller bearing. The contribution from the hydrodynamic bearing can be modeled as viscous damping[1] and the constitutive relation governing the constraint moment is given by equation A-11.

$$M_V^H = c_V (p_F - p_A) \tag{A-11}$$

The frictional moment at a roller bearing is proportional to the normal force acting on the bearing. Normal force at the bearing of a split bodied projectile is directly related to the axial aerodynamic coefficients of the forward and aft bodies. The contribution to the constraint moment from a roller bearing[2] is given by equation A-12. To remove the effects of either bearing from the model, set the respective coefficient to zero.

$$M_V^R = C_{RB} |F_{CX}| sign(p_F - p_A) \tag{A-12}$$

---

[1] Close, C. M., and D. K. Frederick. *Modeling and Analysis of Dynamic Systems.* New York, NY: John Wiley and Sons, 1995.

[2] Bolz, R. E., and G. L. Tuve. CRC Handbook of Tables for Applied Engineering Science. OH: CRC Press, 1973.

Once the final constraint moment is known, the fixed plane $\vec{i}_n$ components of equations 4 and 5 are the forward and aft body roll dynamic equations. These two individual equations, in conjunction with the fixed plane $\vec{j}_n$ and $\vec{k}_n$ equations, resulting from a sum of equations 4 and 5, can be assembled to represent the entire set of rotational dynamics. Equation 4, from the main body of this report, is restated below to demonstrate this point.

$$\begin{bmatrix} I_{1,1} & I_{1,2} & I_{1,3} & I_{1,4} \\ I_{2,1} & I_{2,2} & I_{2,3} & I_{2,4} \\ I_{3,1} & I_{3,2} & I_{3,3} & I_{3,4} \\ I_{4,1} & I_{4,2} & I_{4,3} & I_{4,4} \end{bmatrix} \begin{Bmatrix} \dot{p}_F \\ \dot{p}_A \\ \dot{q} \\ \dot{r} \end{Bmatrix} = \begin{Bmatrix} g_{F1} - M_V \\ g_{A1} + M_V \\ M_2 - S_2^* \\ M_3 - S_3^* \end{Bmatrix}$$

The effective inertia matrix is a 4×4 matrix that is a combination of the inertia matrices of both the forward and aft bodies. As an aid in developing a formula for the effective inertia matrix, define the following intermediate matrices.

$$I_A^* = \bar{I}_A - \tilde{I}_A \tag{A-13}$$

$$\bar{I}_A = T_A{}^T I_A T_A \tag{A-14}$$

$$\tilde{I}_A = m_A S_{RA} S_{RA} \tag{A-15}$$

$$I_F^* = \bar{I}_F - \tilde{I}_F \tag{A-16}$$

$$\bar{I}_F = T_F{}^T I_F T_F \tag{A-17}$$

$$\tilde{I}_F = m_F S_{RF} S_{RF} \ , \tag{A-18}$$

where

$$T_F = \begin{bmatrix} 1 & 0 & 0 \\ 0 & c_{\phi_F} & s_{\phi_F} \\ 0 & -s_{\phi_F} & c_{\phi_F} \end{bmatrix} \tag{A-19}$$

$$T_A = \begin{bmatrix} 1 & 0 & 0 \\ 0 & c_{\phi_A} & s_{\phi_A} \\ 0 & -s_{\phi_A} & c_{\phi_A} \end{bmatrix} \tag{A-20}$$

$$S_{RF} = \begin{bmatrix} 0 & -r_{fz} & r_{fy} \\ r_{fz} & 0 & -r_{fx} \\ -r_{fy} & r_{fx} & 0 \end{bmatrix} \tag{A-21}$$

$$S_{RA} = \begin{bmatrix} 0 & -r_{az} & r_{ay} \\ r_{az} & 0 & -r_{ax} \\ -r_{ay} & r_{ax} & 0 \end{bmatrix} \tag{A-22}$$

Using equations A-13, A-16, A-11, and A-12, elements of the effective inertia matrix can now be formed.

$$I_{1,1} = I^*_{F_{1,1}} + M_{FF_{1,1}} \tag{A-23}$$

$$I_{1,2} = M_{FA_{1,1}} \tag{A-24}$$

$$I_{1,3} = I^*_{F_{1,2}} + M_{FF_{1,2}} + M_{FA_{1,2}} \tag{A-25}$$

$$I_{1,4} = I^*_{F_{1,3}} + M_{FF_{1,3}} + M_{FA_{1,3}} \tag{A-26}$$

$$I_{2,1} = M_{AF_{1,1}} \tag{A-27}$$

$$I_{2,2} = I^*_{A_{1,1}} - M_{AA_{1,1}} \tag{A-28}$$

$$I_{2,3} = I^*_{A_{1,2}} - M_{AA_{1,2}} - M_{AF_{1,2}} \tag{A-29}$$

$$I_{2,4} = I^*_{A_{1,3}} - M_{AA_{1,3}} - M_{AF_{1,3}} \tag{A-30}$$

$$I_{3,1} = I^*_{F_{2,1}} \tag{A-31}$$

$$I_{3,2} = I^*_{A_{2,1}} \tag{A-32}$$

$$I_{3,3} = I^*_{F_{2,2}} + I^*_{A_{2,2}} \tag{A-33}$$

$$I_{3,4} = I^*_{F_{2,3}} + I^*_{A_{2,3}} \tag{A-34}$$

$$I_{4,1} = I^*_{F_{3,1}} \tag{A-35}$$

$$I_{4,2} = I^*_{A_{3,1}} \tag{A-36}$$

$$I_{4,3} = I^*_{F_{3,2}} + I^*_{A_{3,2}} \tag{A-37}$$

$$I_{4,4} = I^*_{F_{3,3}} + I^*_{A_{3,3}} \tag{A-38}$$

Two elements of the right-hand side vector of equation 4, from the main body of this report, are given by equations A-39 and A-40.

$$g_{F_1} = \begin{bmatrix} 1 & 0 & 0 \end{bmatrix} \begin{bmatrix} M_F - S^*_F - M_{F0} \end{bmatrix} \tag{A-39}$$

$$g_{A_1} = [1 \quad 0 \quad 0][M_A - S_A^* + M_{A0}] \tag{A-40}$$

The vectors $\vec{S}_A^*$ and $\vec{S}_F^*$ in equation 89, from the main body of this report, and equation A-1 are given by equations A-41 and A-42.

$$S_A^* = \overline{S}_A - \widetilde{S}_A \tag{A-41}$$

$$\overline{S}_A = \left[T_A{}^T I_A \dot{T}_A + T_A{}^T S_A I_A T_A\right]\begin{Bmatrix} p_a \\ q \\ r \end{Bmatrix} \tag{A-42}$$

$$\widetilde{S}_A = \left[\widetilde{I}_A T_A{}^T \dot{T}_A + m_A S_{RA} S_{WA} S_{RA}\right]\begin{Bmatrix} p_a \\ q \\ r \end{Bmatrix} \tag{A-43}$$

$$S_F^* = \overline{S}_F - \widetilde{S}_F \tag{A-44}$$

$$\overline{S}_F = \left[T_F{}^T I_F \dot{T}_F + T_F{}^T S_F I_F T_F\right]\begin{Bmatrix} p_f \\ q \\ r \end{Bmatrix} \tag{A-45}$$

$$\widetilde{S}_F = \left[\widetilde{I}_F T_F{}^T \dot{T}_F + m_F S_{RF} S_{WF} S_{RF}\right]\begin{Bmatrix} p_f \\ q \\ r \end{Bmatrix}, \tag{A-46}$$

where

$$S_F = \begin{bmatrix} 0 & s_{\phi_F} q - c_{\phi_F} r & c_{\phi_F} q + s_{\phi_F} r \\ c_{\phi_F} r - s_{\phi_F} q & 0 & -p_F \\ -c_{\phi_F} q - s_{\phi_F} r & p_F & 0 \end{bmatrix}$$

$$S_A = \begin{bmatrix} 0 & s_{\phi_A} q - c_{\phi_A} r & c_{\phi_A} q + s_{\phi_A} r \\ c_{\phi_A} r - s_{\phi_A} q & 0 & -p_A \\ -c_{\phi_A} q - s_{\phi_A} r & p_A & 0 \end{bmatrix}$$

$$S_{WF} = \begin{bmatrix} 0 & -r & q \\ r & 0 & -p_F \\ -q & p_F & 0 \end{bmatrix}$$

$$S_{WA} = \begin{bmatrix} 0 & -r & q \\ r & 0 & -p_A \\ -q & p_A & 0 \end{bmatrix}$$

$$\dot{T}_F = \begin{bmatrix} 0 & 0 & 0 \\ 0 & -(p_F + t_\theta r) s_{\phi_F} & (p_F + t_\theta r) c_{\phi_F} \\ 0 & -(p_F + t_\theta r) c_{\phi_F} & -(p_F + t_\theta r) s_{\phi_F} \end{bmatrix}$$

$$\dot{T}_A = \begin{bmatrix} 0 & 0 & 0 \\ 0 & -(p_A + t_\theta r) s_{\phi_A} & (p_A + t_\theta r) c_{\phi_A} \\ 0 & -(p_A + t_\theta r) c_{\phi_A} & -(p_A + t_\theta r) s_{\phi_A} \end{bmatrix}$$

Other unknown terms on the right-hand side of equation A-4 include components of the vectors $\vec{M}$ and $\vec{S}^*$. These vectors are described below.

$$S^* = S_F^* + S_A^* = \begin{Bmatrix} S_1^* \\ S_2^* \\ S_3^* \end{Bmatrix} \tag{A-47}$$

$$M = M_F + M_A = \begin{Bmatrix} M_1 \\ M_2 \\ M_3 \end{Bmatrix} \tag{A-48}$$

NO. OF COPIES ORGANIZATION

2 DEFENSE TECHNICAL INFORMATION CENTER
DTIC DDA
8725 JOHN J KINGMAN RD
STE 0944
FT BELVOIR VA 22060-6218

1 HQDA
DAMO FDQ
D SCHMIDT
400 ARMY PENTAGON
WASHINGTON DC 20310-0460

1 OSD
OUSD(A&T)/ODDDR&E(R)
R J TREW
THE PENTAGON
WASHINGTON DC 20301-7100

1 DPTY CG FOR RDA
US ARMY MATERIEL CMD
AMCRDA
5001 EISENHOWER AVE
ALEXANDRIA VA 22333-0001

1 INST FOR ADVNCD TCHNLGY
THE UNIV OF TEXAS AT AUSTIN
PO BOX 202797
AUSTIN TX 78720-2797

1 DARPA
B KASPAR
3701 N FAIRFAX DR
ARLINGTON VA 22203-1714

1 NAVAL SURFACE WARFARE CTR
CODE B07 J PENNELLA
17320 DAHLGREN RD
BLDG 1470 RM 1101
DAHLGREN VA 22448-5100

1 US MILITARY ACADEMY
MATH SCI CTR OF EXCELLENCE
DEPT OF MATHEMATICAL SCI
MADN MATH
THAYER HALL
WEST POINT NY 10996-1786

NO. OF COPIES ORGANIZATION

1 DIRECTOR
US ARMY RESEARCH LAB
AMSRL DD
2800 POWDER MILL RD
ADELPHI MD 20783-1197

1 DIRECTOR
US ARMY RESEARCH LAB
AMSRL CS AS (RECORDS MGMT)
2800 POWDER MILL RD
ADELPHI MD 20783-1145

3 DIRECTOR
US ARMY RESEARCH LAB
AMSRL CI LL
2800 POWDER MILL RD
ADELPHI MD 20783-1145

ABERDEEN PROVING GROUND

4 DIR USARL
AMSRL CI LP (BLDG 305)

NO. OF COPIES	ORGANIZATION
3	AIR FORCE RSRCH LAB MUNITIONS DIR AFRL/MNAV G ABATE 101 W EGLIN BLVD STE 219 EGLIN AFB FL 32542
3	ALLEN PETERSON 159 S HIGHLAND DR KENNEWICK WA 99337
1	CDR WL/MNMF D MABRY 101 W EGLIN BLVD STE 219 EGLIN AFB FL 32542-6810
20	DEPT OF MECHL ENGRG M COSTELLO OREGON STATE UNIVERSITY CORVALLIS OR 97331
4	CDR US ARMY ARDEC AMSTA AR CCH J DELORENZO S MUSALI R SAYER P DONADIO PICATINNY ARESENAL NJ 07806-5000
7	CDR US ARMY TANK MAIN ARMAMENT SYSTEM AMCPM TMA D GUZIEWICZ R DARCEY C KIMKER R JOINSON E KOPOAC T LOUZIERIO C LEVECHIA PICATINNY ARESENAL NJ 07806-5000
1	CDR USA YUMA PROV GRND STEYT MTW YUMA AZ 85365-9103

NO. OF COPIES	ORGANIZATION
10	CDR US ARMY TACOM AMCPEO HFM AMCPEO HFM F AMCPEO HFM C AMCPM ABMS AMCPM BLOCKIII AMSTA CF AMSTA Z AMSTA ZD AMCPM ABMS S W DR PATTISON A HAVERILLA WARREN MI 48397-5000
1	DIR BENET LABORATORIES SMCWV QAR T MCCLOSKEY WATERVLIET NY 12189-5000
1	CDR USAOTEA CSTE CCA DR RUSSELL ALEXANDRIA VA 22302-1458
2	DIR US ARMY ARMOR CTR & SCHL ATSB WP ORSA A POMEY ATSB CDC FT KNOX KY 40121
1	CDR US ARMY AMCCOM AMSMC ASR A MR CRAWFORD ROCK ISLAND IL 61299-6000
2	PROGRAM MANAGER GROUND WEAPONS MCRDAC LTC VARELA CBGT QUANTICO VA 22134-5000

NO. OF COPIES	ORGANIZATION
4	COMMANDER US ARMY TRADOC ATCD T ATCD TT ATTE ZC ATTG Y FT MONROE VA 23651-5000
1	NAWC F PICKETT CODE C2774 CLPL BLDG 1031 CHINA LAKE CA 93555
1	NAVAL ORDNANCE STATION ADVNCD SYS TCHNLGY BRNCH D HOLMES CODE 2011 LOUISVILLE KY 40214-5001
1	NAVAL SURFACE WARFARE CTR F G MOORE DAHLGREN DIVISION CODE G04 DAHLGREN VA 22448-5000
1	US MILITARY ACADEMY MATH SCI CTR OF EXCELLENCE DEPT OF MATHEMATICAL SCI MDN A MAJ DON ENGEN THAYER HALL WEST POINT NY 10996-1786
3	DIR SNL A HODAPP W OBERKAMPF F BLOTTNER DIVISION 1631 ALBUQUERQUE NM 87185
3	ALLIANT TECH SYSTEMS C CANDLAND R BURETTA R BECKER 7225 NORTHLAND DR BROOKLYN PARK MN 55428

NO. OF COPIES	ORGANIZATION
3	DIR USARL AMSRL SE RM H WALLACE AMSRL SS SM J EIKE A LADAS 2800 POWDER MILL RD ADELPHI MD 20783-1145
1	OFC OF ASST SECY OF ARMY FOR R&D SARD TR W MORRISON 2115 JEFFERSON DAVIS HWY ARLINGTON VA 22202-3911
2	CDR USARDEC AMSTA FSP A S DEFEO R SICIGNANO PICATINNY ARESENAL NJ 07806-5000
2	CDR USARDEC AMSTA AR CCH A M PALATHINGAL R CARR PICATINNY ARESENAL NJ 07806-5000
5	TACOM ARDEC AMSTA AR FSA K CHIEFA AMSTA AR FS A WARNASCH AMSTA AR FSF W RYBA AMSTA AR FSP S PEARCY J HEDDERICH PICATINNY ARESENAL NJ 07806-5000

NO. OF COPIES	ORGANIZATION
5	CDR US ARMY AMCOM AMSAM RD P JACOBS P RUFFIN AMSAM RD MG GA C LEWIS AMSAM RD MG NC C ROBERTS AMSAM RD ST GD D DAVIS REDSTONE ARSENAL AL 35898-5247
3	CDR US ARMY AVN TRP CMD DIRECTORATE FOR ENGINEERING AMSATR ESW M MAMOUD M JOHNSON J OBERMARK REDSTONE ARESENAL AL 35898-5247
1	DIR US ARMY RTTC STERT TE F TD R EPPS REDSTONE ARESENAL AL 35898-5247
2	STRICOM AMFTI EL D SCHNEIDER R COLANGELO 12350 RESEARCH PKWY ORLANDO FL 32826-3276
1	CDR OFFICE OF NAVAL RES CODE 333 J GOLDWASSER 800 N QUINCY ST RM 507 ARLINGTON VA 22217-5660
1	CDR US ARMY RES OFFICE AMXRO RT IP TECH LIB PO BOX 12211 RESEARCH TRIANGLE PARK NJ 27709-2211

NO. OF COPIES	ORGANIZATION
4	CDR US ARMY AVN TRP CMD AVIATION APPLIED TECH DIR AMSATR TI R BARLOW E BERCHER T CONDON B TENNEY FT EUSTIS VA 23604-5577
3	CDR NAWC WEAPONS DIV CODE 543400D S MEYERS CODE C2744 T MUNSINGER CODE C3904 D SCOFIELD CHINA LAKE CA 93555-6100
1	CDR NSWC CRANE DIVISION CODE 4024 J SKOMP 300 HIGHWAY 361 CRANE IN 47522-5000
1	CDR NSWC DAHLGREN DIV CODE 40D J BLANKENSHIP 6703 WEST HWY 98 PANAMA CITY FL 32407-7001
1	CDR NSWC J FRAYSEE D HAGEN 17320 DAHLGREN RD DAHLGREN VA 22448-5000

NO. OF COPIES	ORGANIZATION
5	CDR NSWC INDIAN HEAD DIV CODE 40D D GARVICK CODE 4110C L FAN CODE 4120 V CARLSON CODE 4140E H LAST CODE 450D T GRIFFIN 101 STRAUSS AVE INDIAN HEAD MD 20640-5000
1	CDR NSWC INDIAN HEAD DIV LIBRARY CODE 8530 BLDG 299 101 STRAUSS AVE INDIAN HEAD MD 20640
2	US MILITARY ACADEMY MATH SCI CTR OF EXCELLENCE DEPT OF MATHEMATICAL SCI MDN A MAJ D ENGEN R MARCHAND THAYER HALL WEST POINT NY 10996-1786
3	CDR US ARMY YUMA PG STEYP MT AT A A HOOPER STEYP MT EA YUMA AZ 85365-9110
6	CDR NSWC INDIAN HEAD DIV CODE 570D J BOKSER CODE 5710 L EAGLES J FERSUSON CODE 57 C PARIS CODE 5710G S KIM CODE 5710E S JAGO 101 STRAUSS AVE ELY BLDG INDIAN HEAD MD 20640-5035

NO. OF COPIES	ORGANIZATION
1	BRUCE KIM MICHIGAN STATE UNIVERSITY 2120 ENGINEERING BLDG EAST LANSING MI 48824-1226
2	INDUSTRIAL OPERATION CMD AMFIO PM RO W MCKELVIN MAJ BATEMAN ROCK ISLAND IL 61299-6000
3	PROGRAM EXECUTIVE OFFICER TACTICAL AIRCRAFT PROGRAMS PMA 242 1 MAJ KIRBY R242 PMA 242 33 R KEISER (2 CPS) 1421 JEFFERSON DAVIS HWY ARLINGTON VA 22243-1276
1	CDR NAVAL AIR SYSTEMS CMD CODE AIR 471 A NAKAS 1421 JEFFERSON DAVIS HWY ARLINGTON VA 22243-1276
4	ARROW TECH ASSOCIATES INC R WHYTE A HATHAWAY H STEINHOFF 1233 SHELBOURNE RD SUITE D8 SOUTH BURLINGTON VT 05403
3	US ARMY AVIATION CTR DIR OF COMBAT DEVELOPMENT ATZQ CDM C B NELSON ATZQ CDC C T HUNDLEY ATZQ CD G HARRISON FORT RUCKER AL 36362

NO. OF COPIES ORGANIZATION

ABERDEEN PROVING GROUND

3 CDR
USA ARDEC
AMSTA AR FSF T
R LIESKE
J WHITESIDE
J MATTS
BLDG 120

1 CDR
USA TECOM
AMSTE CT
T J SCHNELL
RYAN BLDG

3 CDR
USA AMSAA
AMXSY EV
G CASTLEBURY
R MIRABELLE
AMXSY EF
S MCKEY

58 DIR USARL
AMSRL WM
I MAY
T ROSENBERGER
AMSRL WM BA
W HORST JR
W CIEPELLA
AMSRL WM BE
M SCHMIDT
AMSRL WM BA
F BRANDON
T BROWN (5 CPS)
L BURKE
J CONDON
B DAVIS
T HARKINS (5 CPS)
D HEPNER
V LEITZKE
M HOLLIS
A THOMPSON

NO. OF COPIES ORGANIZATION

ABERDEEN PROVING GROUND (CONTD)

AMSRL WM BB
B HAUG
AMSRL WM BC
J GARNER
AMSRL WM BD
B FORCH
AMSRL WM BF
J LACETERA
P HILL
AMSRL WM BR
C SHOEMAKER
J BORNSTEIN
AMSRL WM BA
G BROWN
B DAVIS
T HARKINS
D HEPNER
A THOMPSON
J CONDON
W DAMICO
F BRANDON
AMSRL WM BC
P PLOSTINS (4 CPS)
G COOPER
B GUIDOS
J SAHU
M BUNDY
K SOENCKSEN
D LYON
A HORST
I MAY
J BENDER
J NEWILL
AMSRL WM BC
V OSKAY
S WILKERSON
W DRYSDALE
R COATES
A MIKHAL
J WALL

REPORT DOCUMENTATION PAGE

Form Approved
OMB No. 0704-0188

1. AGENCY USE ONLY *(Leave blank)*	2. REPORT DATE	3. REPORT TYPE AND DATES COVERED
	February 2000	Final, Jun 97 - May 98

4. TITLE AND SUBTITLE
Linear Theory of a Dual-Spin Projectile in Atmospheric Flight

5. FUNDING NUMBERS
DAAL01-98M00-33

6. AUTHOR(S)
Mark F. Costello* and Allen A. Peterson**

7. PERFORMING ORGANIZATION NAME(S) AND ADDRESS(ES)
Department of Mechanical Engineering
Oregon State University
Corvallis, OR 97331

8. PERFORMING ORGANIZATION REPORT NUMBER

9. SPONSORING/MONITORING AGENCY NAMES(S) AND ADDRESS(ES)
U.S. Army Research Laboratory
ATTN: AMSRL-WM-BC
Aberdeen Proving Ground, MD 21005-5066

10.SPONSORING/MONITORING AGENCY REPORT NUMBER
ARL-CR-448

11. SUPPLEMENTARY NOTES
*Assistant Professor, Member AIAA
**Graduate Research Assistant

12a. DISTRIBUTION/AVAILABILITY STATEMENT
Approved for public release; distribution is unlimited.

12b. DISTRIBUTION CODE

13. ABSTRACT ***(Maximum 200 words)***

The equations of motion for a dual-spin projectile in atmospheric flight are developed and subsequently utilized to solve for angle of attack and swerving dynamics. A combination hydrodynamic and roller bearing couples forward and aft body roll motions. Using a modified projectile linear theory developed for this configuration, it is shown that the dynamic stability factor, S_D, and the gyroscopic stability factor, S_G, are altered compared to a similar rigid projectile, due to new epicyclic fast and slow arm equations. Swerving dynamics including aerodynamic jump are studied using the linear theory.

14. SUBJECT TERMS
Flight dynamics, Dual-spin, Projectile

15. NUMBER OF PAGES
52

16. PRICE CODE

17. SECURITY CLASSIFICATION OF REPORT	18. SECURITY CLASSIFICATION OF THIS PAGE	19. SECURITY CLASSIFICATION OF ABSTRACT	20. LIMITATION OF ABSTRACT
UNCLASSIFIED	UNCLASSIFIED	UNCLASSIFIED	UL

INTENTIONALLY LEFT BLANK.

USER EVALUATION SHEET/CHANGE OF ADDRESS

This Laboratory undertakes a continuing effort to improve the quality of the reports it publishes. Your comments/answers to the items/questions below will aid us in our efforts.

1. ARL Report Number/Author ARL-CR-448 (Costello [POC: P. Plostins]) Date of Report February 2000

2. Date Report Received _____

3. Does this report satisfy a need? (Comment on purpose, related project, or other area of interest for which the report will be used.) _____

4. Specifically, how is the report being used? (Information source, design data, procedure, source of ideas, etc.) _____

5. Has the information in this report led to any quantitative savings as far as man-hours or dollars saved, operating costs avoided, or efficiencies achieved, etc? If so, please elaborate. _____

6. General Comments. What do you think should be changed to improve future reports? (Indicate changes to organization, technical content, format, etc.) _____

CURRENT ADDRESS

_____
Organization

_____
Name E-mail Name

_____
Street or P.O. Box No.

_____
City, State, Zip Code

7. If indicating a Change of Address or Address Correction, please provide the Current or Correct address above and the Old or Incorrect address below.

OLD ADDRESS

_____
Organization

_____
Name

_____
Street or P.O. Box No.

_____
City, State, Zip Code

(Remove this sheet, fold as indicated, tape closed, and mail.)

(DO NOT STAPLE)